Vietnam Journal of Catalysis and Adsorption, 10 – issue 2 (2021) 49-53

Vietnam Journal of Catalysis and Adsorption
Tạp chí xúc tác và hấp phụ Việt Nam

http://chemeng.hust.edu.vn/jca/

Synthesis of g-C_3N_4/$InVO_4$ materials as novel photocatalysts for degradation of antibiotics under visible light

Mai Hung Thanh Tung[1*], Thanh Dong-Pham[2], Nguyen Tri Quoc[3], Do Minh The[4], Tran Thi Thu Phuong[4], Tran Thi Thu Hien[4], Nguyen Thi Phuong Le Chi[4], Phan Thi Dieu[4], Nguyen Thi Dieu Cam[4]

[1] Chemical Engineering, Ho Chi Minh City University of Food Industry, 140 Le Trong Tan, Ho Chi Minh City, Viet Nam
[2] VNU Key Laboratory of Advanced Materials for Green Growth, VNU University of Science, Vietnam National University, Hanoi, 334 Nguyen Trai, Thanh Xuan, Hanoi,Viet Nam
[3] Mien Trung industry and trade college, Viet Nam, 261 Nguyen Tat Thanh, Tuy Hoa City, Phu Yen, Viet Nam
[4] Faculty of Natural Sciences , Quy Nhon University, 170 An Duong Vuong, Quy Nhon City, Binh Dinh, Viet Nam
**Email: nguyenthidieucam@qnu.edu.vn*

ARTICLE INFO

Received: 15/02/2021
Accepted: 30/4/2021

Keywords:
Graphitic carbon nitride, indium vanadate, photocatalyst; photodegradation, antibiotics

ABSTRACT

Novel g-C_3N_4/$InVO_4$ materials were synthesized by a fabricated via hydrothermal and heating methods. The physicochemical properties of the photocatalysts were investigated by X-ray diffraction (XRD), infrared spectroscopy (IR), Photoluminescence spectroscopy (PL), UV-Vis diffuse reflectance spectroscopy (UV-Vis-DRS) and Energy dispersive X-ray spectroscopy (EDX). The photocatalytic performances were evaluated by degradation of tetracycline (TC). The g-C_3N_4/$InVO_4$ composite at a weight ratio of 10 % exhibited the most excellent photocatalytic activity for TC degradation under visible irradiation which was more active than that of pure components.

Introduction

Semiconductor photocatalysis technology has been received keen interest in the past few decades, due to energy saving, absence of secondary pollution and efficient photocatalytic activity for environmental pollution treatment area with the utilization of solar energy [1-4]. TiO_2 owning to its superior redox ability, low cost and nontoxicity as a main photocatalyst has been widely studied and successfully implemented commercial. However, the wide-band gap semiconductor photocatalyst with 3.2 eV only absorbing UV-light is a significant drawback for practical application in environment remediation [1, 2]. Therefore, many attempts have been made to explore the photocatalysts responsive to visible light.

In recent years, the narrow band gap of 2.7 eV of the graphitic carbon nitride (g-C_3N_4) nanomaterial makes it respond to visible light with the wavelength longer than 400 nm. The g-C_3N_4 exhibits excellent photocatalytic performance for degrading organic pollutants under visible light [5, 6]. Addition, g-C_3N_4 can be simply prepared by the thermal condensation of several low-cost nitrogen-rich precursors such as dicyandiamide, melamine, urea,... which make it a more accessible and promising photocatalyst. However, the photocatalytic activity of individual g-C_3N_4 is limited, in which the photoaction suffers from low conversion efficiency due to the fast recombination of photogenerated hole - electron pairs [7 - 9]. The effectiveness of g-C_3N_4 hybridized with others semiconductors is an effectively method to reduce the

https://doi.org/10.51316/jca.2021.027

charges recombination rate for enhancing photocatalytic performance.

Besides of g-C_3N_4, $InVO_4$ as an novel stable and non-toxic semiconductor material, has attracted considerable interest because of its high response to visible light [10-12]. However, the photocatalytic efficiency of pure $InVO_4$ is not high due to its poor adsorptive performance and the difficulty in migrating photogenerated charge carriers [13]. It has been reported that the values of the conduction band and the valence band levels of $InVO_4$ are 0.32 and 2.75 eV, respectively, both of which are lower than that of g-C_3N_4 [14, 15]. Hence, the $InVO_4$ hybridized with g-C_3N_4 may be more helpful for the charge carriers transfer and separation at the heterojunction surface, consequently improving photocatalytic performance [14, 15].

In the present work, we intend to the development of coupling g-C_3N_4 with $InVO_4$ as a high-performance visible light photocatalyst. The well aligned straddling band structures in hybrids can restrain the photoinduced charge recombination and enhance the transfer of electron-hole pairs, which improves photocatalytic activity for photodegradation organic pollutants. The degradation of tetracycline as a model pollutant under visible light to evaluate photocatalytic activity of g-C_3N_4/$InVO_4$.

Experimental

Photocatalyst synthesis

1 g of urea ($(NH_2)_2CO$) was ground for 15 min to obtain finely powder, which was continuously calcined for 2 h at 530 °C to synthesize g-C_3N_4. To synthesize different mass ratios g-C_3N_4/$InVO_4$ photocatalysts, 0.81 g g-C_3N_4 and 0.162 g NH_4VO_3 were mixed in the 30 mL of deionized water and followed by vigorous stirring 4 h for a uniform suspension. At the same time, 0.572 g $In(NO_3)_3.4.5.H_2O$ solid was dissolved in 3 mL of HNO_3 (1 M) to obtain a clear suspension. The solution was added rapidly to the suspension and soon afterwards stirred for additional 4 h at room temperature. After carefully adjusting the pH value of 4 using NaOH solution (1 M), the mixed solution was transferred into a Teflon-lined steel autoclave, which was heated in an oven at 150 ^oC for 24 h. At last, the obtained product was collected and washed with ethanol and distilled water several times, and dried at 80 ^oC for 2 h. The synthesized materials were named g-C_3N_4/$InVO_4$-x, which X were the weight ratios of the used g-C_3N_4 to the used $InVO_4$ (X = 5, 10, and 15 %). The pure $InVO_4$ sample was fabricated under the same conditions in the absence of g-C_3N_4 powder.

Characterization methods

The prepared materials were carefully analyzed by an X-ray diffractometer (D8 – Advance 5005) to investigate their microstructure. UV–vis absorption spectra of these photocatalysts have been conducted on a UV – Visible spectrophotometer (3101PC Shimadzu). Infrared spectroscopy was recorded on an 760 IR spectrometer (Nicolet-USA). Photoluminescence spectra (PL) were carried out on a Fluoromax-4-type spectrophotometer (Jobin–Yvon Co, France). Energy dispersive X-ray spectroscopy was determined on a S-4800 spectrophotometer (Hitachi – Japan).

Degradation experiments: To assess the photocatalytic degradation efficiency, 0.1 g synthesized material was put in 500 mL of a 200 mL tetracycline (10 mg/L) stored in a dark cover beaker using as reactor. Then, the solution was constantly stirred for 120 min to get the adsorption–desorption equilibrium on photocatalyst surface. After that, the reactor was irradiated by visible light produced from 30 W (SBNL-830). At interval time of 30 min, 5 mL solution was withdrawn and filtered to analyze remained tetracycline using a UV-Vis spectrometer to measure their degradation properties at 355 nm (UV 1800, Shimadzu).

Results and discussion

Material properties

XRD patterns of the prepared g-C_3N_4, $InVO_4$ and g-C_3N_4/$InVO_4$-x were shown in Figure. 1. The obtained XRD pattern of the g-C_3N_4 indicated that two characteristic diffraction peaks of pure g-C_3N_4 observed at 13.1 and 27.4^o can be indexed as the (100) and (002) diffraction planes of graphite-like carbon nitride, respectively (JCPDS 87-1526) [5, 6]. While for pure $InVO_4$, the characteristic peaks at 18.6, 20.8, 23.0, 31.1, 33.2, 35.2, 42.0 and 46.9 are observed, which can be indexed to (110), (020), (111), (200), (122), (130), (202) and (222) crystal planes of $InVO_4$ (JCPDS 48-0898) [16]. For g-C_3N_4/$InVO_4$ composites, the main diffraction peaks of g-C_3N_4 and $InVO_4$ materials did not change obviously, with the increase of weight ratios of 5, 10 and 15%, the peak intensity of g-C_3N_4 is highest at weight ratio of 15%, this peak is weaker for g-C_3N_4/$InVO_4$-10 and C_3N_4/$InVO_4$-5, indicating that the fabrication process did not destroy the main structure of both components.

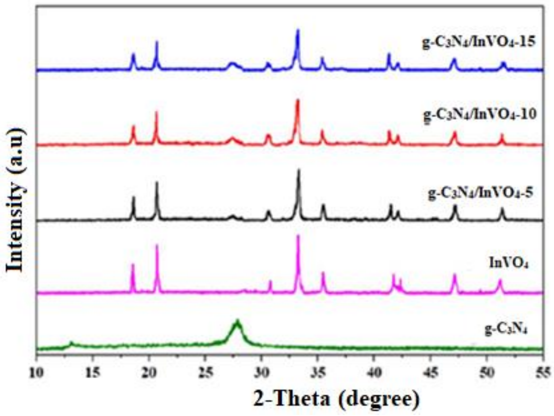

Figure 1: XRD patterns of $g\text{-}C_3N_4$, $InVO_4$ and $g\text{-}C_3N_4/InVO_4$-x

The UV-Vis-DRS was carried out to investigate the optical absorption of the as-prepared samples. The band gap energies of the obtained photocatalysts was estimated by using the Tauc plot, combining with the Kubelka–Munk method. In the Tauc plot, a linear fit was drawn from the transformed curves to the photon energy axis and the energy value at the point of intersection of the line and the horizontal axis was the band gap energy of the materials. The obtained results indicate that the visible light absorption of the prepared $InVO_4$ material was higher than visible light absorption of the prepared $g\text{-}C_3N_4$. This was because the band-gap energy of the $InVO_4$ (2.45 eV) materials was lower than that of the $g\text{-}C_3N_4$ (2.75 eV) (Figure. 2). The optical absorption spectra also show that visible light absorption of the prepared $g\text{-}C_3N_4/InVO_4$ materials were better than that of single $g\text{-}C_3N_4$ and $InVO_4$ materials. The $g\text{-}C_3N_4/InVO_4$ material corresponding to 10% weight percentage of $g\text{-}C_3N_4/InVO_4$ exhibited the highest visible light absorption among prepared composite materials. The calculated band-gap energies of the $g\text{-}C_3N_4/InVO_4$-5, $g\text{-}C_3N_4/InVO_4$-10 and $g\text{-}C_3N_4/InVO_4$ were 2.68, 2.55 and 2.62 eV, respectively.

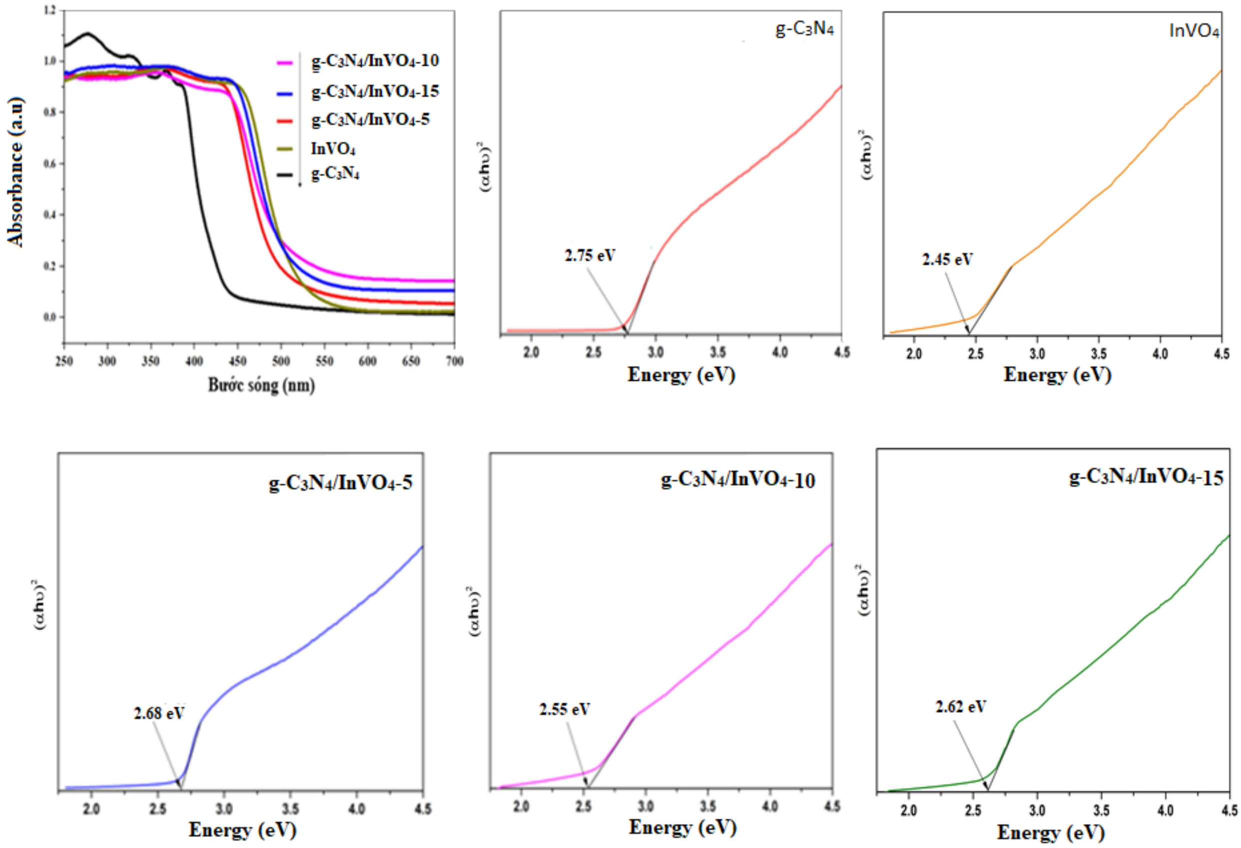

Figure 2: UV–Vis diffuse reflectance spectra and the plots of $(\alpha h\nu)^2$ versus energy (hν) for the band gap energy of $g\text{-}C_3N_4$, $InVO_4$ and $g\text{-}C_3N_4/InVO_4$-x

Synthesized materials were also further analyzed by an a photoluminescence emission spectrophotometer to determine their optical properties. The $g\text{-}C_3N_4$, $InVO_4$ and $g\text{-}C_3N_4/InVO_4$-x PL spectra were shown in Figure 3. Pure $g\text{-}C_3N_4$ and $InVO_4$ had strong PL peak intensity. When $g\text{-}C_3N_4$ was combined with the $InVO_4$, the $g\text{-}C_3N_4/InVO_4$ heterojunction displayed lower intensity. The PL spectra areusually utilized to determine charge (e- and h+) separation efficiency. A lower PL peak usually corresponds to lower charge recombination rate or lower charge separation efficiency. Thus, the formation of heterojunction successfully solved the problem of easy recombination of photogenerated charges of single photocatalysts. g-C_3N_4/$InVO_4$-10 shows a lowest luminescence emission among prepared composites

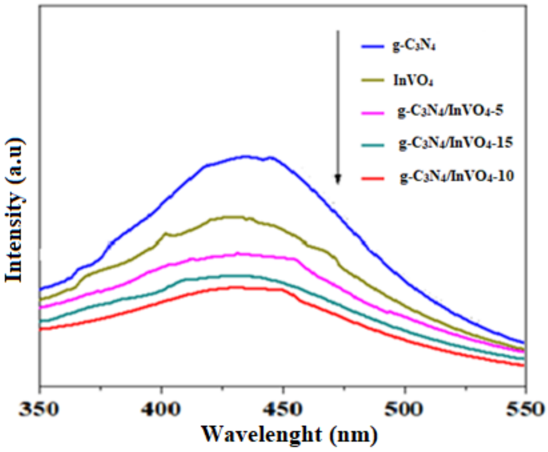

Figure 3: PL spectra of g-C_3N_4, $InVO_4$ and g-C_3N_4/$InVO_4$-x materials

The IR spectra of the g-C_3N_4, $InVO_4$ and g-C_3N_4/$InVO_4$-10 material are shown in Figure. 4. In the IR spectrum of g-C_3N_4, The absorption peak at 1662 cm^{-1} corresponds to C-N stretching vibrations, and peaks at 1240 and 1408 cm^{-1} are attributable to aromatic C=N breathing modes.

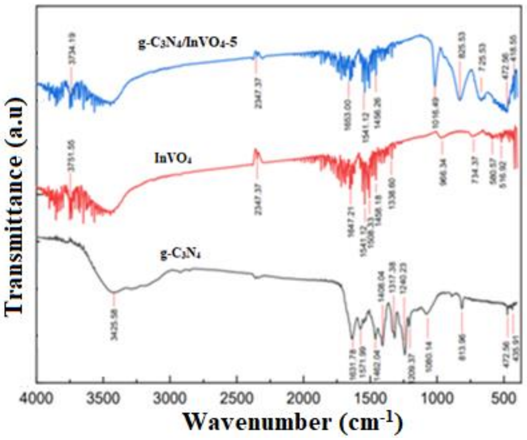

Figure 4: IR spectra of $InVO_4$, g-C_3N_4 and $InVO_4$/g-C_3N_4 materials

The adsorption peak at 813 cm-1 belongs to the breathing mode of triazine units [17]. The peak at about 472 cm-1 is assigned to the V–O–V band and the strong peak at 735 cm-1 indicates the existence of VO_4^{3-} groups. And peak at 956 cm-1 correspond to the characteristic vibration V–O, respectively [18, 19]. In the case of the g-C_3N_4/$InVO_4$-10 composite, most of the characteristic peaks of g-C_3N_4 were obscured after the introduction of $InVO_4$ composites and the peak at 813 cm^{-1} corresponds to the breathing mode of triazine units in g-C_3N_4 was noted at 825 cm^{-1}, indicating the coexistence of these two semiconductors.

Energy dispersive X-ray spectroscopy was used to determine the elemental composition of the synthesized g-C_3N_4/$InVO_4$-10 material in Figure. 5. The EDX spectrum of g-C_3N_4/$InVO_4$-10 demonstrates the existence of C, N, In, V and O elements without any other impurities.

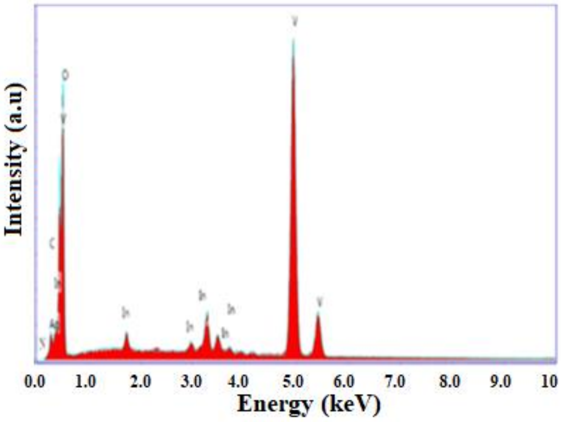

Figure 5: EDS spectra of g-C_3N_4/$InVO_4$ material

Photocatalytic activities

The photocatalytic activity of the C_3N_4/$InVO_4$-10 samples were determined by degradation of TC in water under visible light (SBNL-830 led lamp light sources). For comparison, the photocatalytic activity of g-C_3N_4 and $InVO_4$ is also presented. Figure 6 indicates that the photocatalytic activity of g-C_3N_4/$InVO_4$–x was better than those of g-C_3N_4 and $InVO_4$. This was because the excitation of the electron from the HOMO to the LUMO orbital of $InVO_4$ could be directly injected into the valence band of g-C_3N_4, leading to a significant decrease in the electron–hole recombination for $InVO_4$ in the composites. Hence, this may contribute to the significant enhancement of the photocatalytic reactivity of g-C_3N_4/$InVO_4$–x. Figure 6 also shows that the g-C_3N_4/$InVO_4$ optimal weight ratio enhancing photocatalytic conversion of TC is 10 wt.% with the degradation efficiency is 79.61%. The obtained result is consistent with the characterized properties and reveal higher degradation efficiency compared to other study [15]. There is a certain limit on g-C_3N_4/$InVO_4$ weight ratio leading to enhancement in its photocatalytic activity. According to Wang's report, in

TC degradation process, there were three possible products of degradation pathway [20].

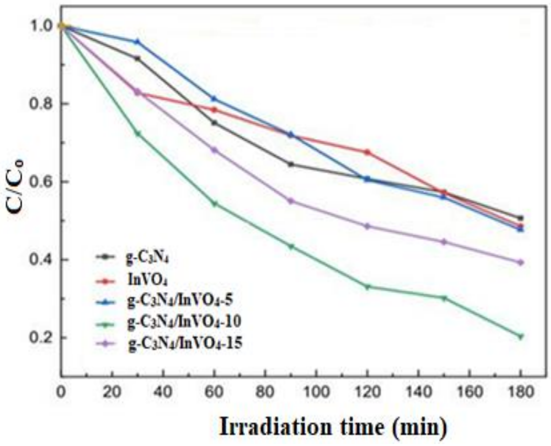

Figure 6: Conversion of TC using g-C_3N_4, $InVO_4$ and g-$C_3N_4/InVO_4$–x under visible light source

Conclusion

We succesfully synthetized a series of g-$C_3N_4/InVO_4$ visible-light-induced composites by a via hydrothermal and heating methods. The g-$C_3N_4/InVO_4$ photocatalysts possess significantly improved visible light photocatalytic activity for TC degradation compared with g-C_3N_4 and $InVO_4$. The g-$C_3N_4/InVO_4$-10 (10 wt%) exhibits the highest photocatalytic performance. The enhancement of photocatalytic efficiency under visible light is mainly attributed to the match of conduction and valence band levels between the g-C_3N_4 and the $InVO_4$, which can induce the high separation of photo-generated electron–hole pairs in the heterojunction system.

Acknowledgments

This research is funded by Vietnam National Foundation for Science and Technology Development (NAFOSTED) under grant number 104.99-2019.49.

References

1. R. Jaiswal, J. Bharambe, N. Patel, A. Dashora, D. C. Kothari, A. Miotello, Applied Catalysis B: Environmental 168 (2015) 333-341. http://dx.doi.org/10.1016/j.apcatb.2014.12.053
2. M. Pelaez, N. T. Nolan, S. C. Pillai, M. K. Seery, P. Falaras, A. G. Kontos, P. S. M. Dunlop, J. W. J. Hamilton, J. A. Byrne, K. O'Shea, M. H. Entezarig, D. D. Dionysioua, Applied Catalysis B: Environmental,125 (2012) 331–349. https://doi.org/10.1016/j.apcatb.2012.05.036
3. M. Mollavali, C. Falamaki, S. Rohani, International Journal of Hydrogen Energy, 40 (2015) 12239–12252. http://dx.doi.org/10.1016/j.ijhydene.2015.07.069
4. S. J Hong, S. Lee, Jang J. S. Jang, J. S. Lee, Energy Environmental Science, 4 (2011) 1781–1787. doi:10.1039/c0ee00743a
5. J. Xu, H. T. Wu, X. Wang, B. Xue, Y. X. Li and Y. Cao., Physical Chemistry Chemical Physics, 15 (2013) 4510– 4517. http://doi:10.1039/c3cp44402c
6. A. Thomas, A. Fischer, F. Goettmann, M. Antonietti, J. O. Muller, R. Schlogl and J. M. Carlsson., Journal of Material Chemistry, 18 (2018) 4893–4908. http://doi:10.1039/b800274f
7. Z. Zang, M. Wang, W. Cui, H. Sui., RSC Advances 7 (2017) 8167-8177. http://doi:10.1007/s10971-014-3454-x
8. Q. Xie, W. He, S. Liu, C. Li, J. Zhang, P. K. Wong, Chinese Journal of Catalysis, 41 (2020) 140–153. https://doi.org/10.1016/S1872-2067(19)63481-9
9. Y. Song, J. Gu, K. Xia, J. Yi, H. Chen, X. She, Z. Chen, C. Ding, H. Li, H. Xu, Applied Surface Science, 467 (2019) 56-64. https://doi.org/10.1016/j.apsusc.2018.10.118
10. L. Zhang, H. Fu, C. Zhang, Y. Zhu, Journal of Solid State Chemistry 179 (2006) 804-811. http://doi:10.1002/chin.200624017
11. J. Shena, H. Yangab, Q. Shenab, Z. You (2014), Procedia Engineering 94 (2014) 64 – 70. http://doi:10.1016/j.proeng.2013.11.043
12. Y. Wang, G. Z Cao, Journal of Materials Chemistry 17 (2007) 894-899. http://doi:10.1557/proc-0922-u01-06
13. J. Shen, H. Yang, Q. Shen, Y. Feng, Journal of Material Science 48 (2013) 7574-7580. http://doi:10.1007/s10853-013-7573-5
14. B. Hu, F. Cai, T. Chen, M. Fan, C. Song, X. Yan, W. Shi, ACS Applied Materials & Interfaces 7 (2015) 18247-18256. http://doi:10.1021/acsami.5b05715
15. Y. Zengyu, S. Yuxuan, Y. Yang, H. Wang, T. Qin, F. Zhang, Q. Shen, H. Yang, Applied Catalysis B: Environmental 213 (2017) 127-135. http://doi:10.1016/j.apcatb.2017.05.015
16. P. Tang, H. Chen, F. Cao, G. Pan, K. Wang, Advanced Material Resource 284 (2011) 734-737. http://doi:10.4028/www.scientific.net/amr.284-286.734
17. L. Gu, J. Wang, Z. Zou, X. Han, Journal of Hazardous Material 268 (2014) 216–223. http://doi:10.1016/j.jhazmat.2014.01.021
18. Y. X. Zhang, D. Ma, J. Wu, Q. Z Zhang, X.J Xin, N. Bao, Applied Surface Science 353 (2015) 1260–1268. https://doi.org/10.1016/j.apsusc.2015.06.143
19. J. M. Yao, C. K. Lee, S. J. Yang, C. S. Hwang, Journal of Alloys Compound 481 (2009) 740–745. http://doi:10.1016/j.jallcom.2009.03.093